

Chapter 5

Implications of Delay Feedback: Amplitude Death and Other Effects

5.1 Introduction

For a long time, in the study of coupled nonlinear oscillators, the role of delay has often been neglected as unimportant. In many cases this approximation is physically justified and in all the cases it simplifies the mathematics. However, in recent times one has witnessed increased activities to investigate oscillator systems with delay feedback and it has been proved that delay feedback is a veritable black box which can give rise to several interesting and novel phenomena having wide applications, and these cannot be observed in the absence of delay feedback. In this chapter, we will discuss an important time-delay induced phenomenon, namely amplitude death, which has been the center of attraction in recent research on coupled oscillators with delay feedback. In addition, we will also point out some of the other important time-delay induced phenomena observed in coupled oscillators.

5.2 Time-Delay Induced Amplitude Death

The phenomenon of suppression of oscillations (*amplitude death*, see Sec. 5.2.1.1 below for more details) was realized by Bar-Eli [1] in his modeling of chemical oscillations and by Shiino and Frankowicz [2] when they considered the effects on the amplitudes in a large number of coupled limit cycles. But a rigorous and comprehensive study on the nature of amplitudes of two coupled oscillators was made by Aronson et al. [3] followed by other elegant studies extending this to a large system [4–6]. However, the concept of amplitude death has now become an active area of research due to the recent works of Ramana Reddy et al. [7–10] on the effect of time-delay feedback in limit cycle oscillators. They have shown particularly that amplitude death can occur even with zero frequency mismatch among the interacting limit cycle oscillators (identical oscillators) in the presence of time-delay feedback. This is in contrast to the earlier reports on amplitude death where such a state can occur only when there exists a broad dispersion in the natural frequencies of the coupled oscillators and that the coupling strength has to exceed a threshold value so that amplitude death

cannot occur in a collection of identical limit cycle oscillators without delay. In this section, we will discuss the theoretical and experimental investigations of delay induced amplitude death phenomenon in single and two coupled limit cycle oscillators.

5.2.1 Theoretical Study: Single Oscillator

In this section, we will demonstrate the theoretical analysis of existence of delay induced amplitude death phenomenon in single and two coupled limit cycle oscillators and its subsequent extension to N coupled limit cycle oscillators with global and ring coupling configurations.

5.2.1.1 Single Limit Cycle Oscillator with Delay Feedback

Specifically, Ramana Reddy et al. [7–10] have considered a model equation, which represents the dynamics of a single Hopf oscillator that is driven autonomously by a time-delayed feedback term, given by

$$\dot{Z}(t) = (a + i\omega - |Z(t)|^2)Z(t) - KZ(t - \tau), \quad (5.1)$$

where $Z(t) = X + iY$ is a complex quantity, ω is the frequency of oscillation, a is a real constant and $\tau > 0$ is the time-delay of the autonomous feedback term. In the absence of the feedback term (5.1) is often called the Stuart-Landau equation, which exhibits a stable limit cycle of amplitude \sqrt{a} with angular frequency ω . In the absence of time-delay, Eq. (5.1) has a time-asymptotic periodic solution given by $Z(t) = \sqrt{a - K} \exp i\omega t$ for $a > K$. If $a \leq K$, then the origin is the only stable solution; that is, no oscillatory time-asymptotic solution is possible. At $a = K$, the oscillator undergoes a supercritical Hopf bifurcation. Carrying out a linear stability analysis for the above equation around the fixed point $Z = Z^* = 0$, one can straightforwardly obtain the characteristic equation

$$\lambda = a + i\omega - Ke^{-\lambda\tau}, \quad \tau > 0. \quad (5.2)$$

For $\tau = 0$, one can have $\lambda = a + i\omega - K$ and hence the origin is stable for $K > a$. So the critical curve is given in this case by $K = a$. When $\tau \neq 0$, Eq. (5.2) remains a transcendental equation with infinite number of roots. Now, one has to find conditions on K , ω and τ such that real parts of all the roots are negative for stability of the fixed point Z^* . Substituting $\lambda = \alpha + i\beta$, where α and β are real, in Eq. (5.2), one can obtain the real and imaginary parts as

$$\alpha = a - Ke^{-\alpha\tau} \cos(\beta\tau), \quad (5.3)$$

$$\beta = \omega + Ke^{-\alpha\tau} \sin(\beta\tau). \quad (5.4)$$

Following the analysis in Sect. 2.4 in Chap. 2, one can obtain a set of critical curves,

$$\tau_1(n, K) = \frac{2n\pi + \arccos\left(\frac{a}{K}\right)}{\omega + \sqrt{K^2 - a^2}}, \quad n = 0, +1, +2, \dots \quad (5.5a)$$

$$\tau_2(n, K) = \frac{2n\pi - \arccos\left(\frac{a}{K}\right)}{\omega - \sqrt{K^2 - a^2}}, \quad n = +1, +2, +3, \dots \quad (5.5b)$$

Also we get

$$\left. \frac{d\alpha}{d\tau} \right|_{\alpha=0} = \frac{\beta(\beta - \omega)}{[1 - K\tau \cos(\beta\tau)]^2 + [K\tau \sin(\beta\tau)]^2}. \quad (5.6)$$

Hence, from (5.4) and (5.6), one can easily see that

$$\left. \frac{d\alpha}{d\tau} \right|_{\alpha=0} \begin{cases} > 0 & \text{on } \tau_1, \\ > 0 \text{ on } \tau_2 & \text{if } K > f(\omega), \\ = 0 \text{ on } \tau_2 & \text{if } K = f(\omega), \\ < 0 \text{ on } \tau_2 & \text{if } K < f(\omega), \end{cases} \quad (5.7)$$

where $f(\omega) = \sqrt{a^2 + \omega^2}$. The above condition implies that there can be only one stability region if $K > f(\omega)$. On the other hand, there is a possibility of multiple stability regions if $K < f(\omega)$. The numerical plot in Fig. 5.1a of the curves $\tau_1(n, K)$ (represented by continuous curves) and $\tau_2(n, K)$ (represented by discrete curves) reveals that the region between $\tau = 0$ and $\tau = \tau_1(0, K)$ is the only stable region (indicated as the shaded region) possible for small values of ω . However, as the value of ω is increased, so that the condition $K < \sqrt{a^2 + \omega^2}$ is satisfied, the number of stability regions also increases. These regions are specified by $0 \leq \tau < \tau_1(0, K)$ and $\tau_1(n, K) < \tau < \tau_2(n, K)$, where the integer $n > 0$. In Fig. 5.1b the critical

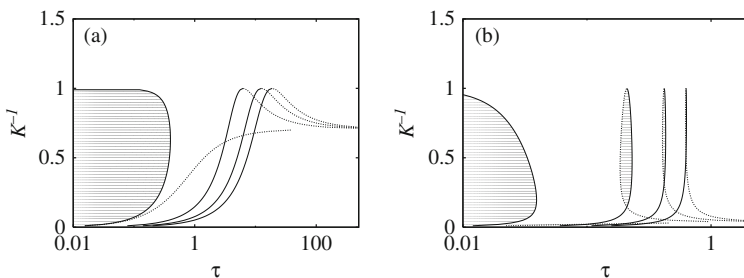


Fig. 5.1 Curves of Eq. (5.5a) and (5.5b). The *solid curves* represent τ_1 for $n = 0, +1, +2, +3$ and *broken curves* represent τ_2 for $n = +1, +2, +3$. **(a)** The region enclosed between the line $\tau = 0$ and the curve $\tau = \tau_1(0, K)$ is the only amplitude death region for $\omega = 1$. **(b)** The region enclosed between the line $\tau = 0$ and the curve $\tau = \tau_1(0, K)$, and that between $\tau_1(n, K)$ and $\tau_2(n, K)$ for $n > 0$ are the multiple amplitude death regions for $\omega = 30$

curves are plotted from Eqs. (5.5a) and (5.5b) for such a large value of ω , namely $\omega = 30$, and the multiple stability regions are represented by shaded regions enclosed between the continuous curves, $\tau_1(n, K)$, and the discrete curves, $\tau_2(n, K)$, for $n > 0$ in addition to that enclosed between the $\tau = 0$ and $\tau = \tau_1(0, K)$ curves. The above collective stability regions have been termed as amplitude death regions or death islands in the $(K - \tau)$ space.

Note that the above analysis shows that when the parameters in (5.1) are such that (i) $K < a$ in the absence of delay ($\tau = 0$), the system has a stable periodic solution $Z = \sqrt{a - K} e^{i\omega t}$, and (ii) in the presence of delay ($\tau \neq 0$), with $K < \sqrt{a^2 + \omega^2}$, this solution becomes unstable, while the fixed point $Z = 0$ becomes stable. This phenomenon is nothing but the amplitude death of the periodic oscillation.

5.2.1.2 Two Delay Coupled Limit Cycle Oscillators

The above analysis has also been extended to a system of two coupled limit cycle oscillators with delay [7–10]. Here, we will briefly describe the existence of delay induced death phenomenon in a set of two delay coupled limit cycle oscillators represented by

$$\dot{Z}_1(t) = (1 + i\omega - |Z_1(t)|^2)Z_1(t) - K [Z_2(t - \tau) - Z_1(t)], \quad (5.8a)$$

$$\dot{Z}_2(t) = (1 + i\omega - |Z_2(t)|^2)Z_2(t) - K [Z_1(t - \tau) - Z_2(t)]. \quad (5.8b)$$

The parameters are the same as discussed above for the case of a single limit cycle oscillator with the delay feedback. Following a linear stability analysis, one can obtain the characteristic equation associated with the equilibrium solution $Z_1 = 0 = Z_2$ for the above delay coupled limit oscillators, Eq. (5.8), as

$$\lambda = 1 - K + i\omega \pm K e^{-\lambda\tau}. \quad (5.9)$$

After simple algebra, one can obtain a set of critical curves,

$$\tau_1(n, K) = \frac{2n\pi + \arccos\left(1 - \frac{1}{K}\right)}{\omega - \sqrt{2K - 1}}, \quad n = 0, +1, +2, \dots \quad (5.10a)$$

$$\tau_2(n, K) = \frac{2n\pi - \arccos\left(1 - \frac{1}{K}\right)}{\omega + \sqrt{2K - 1}}, \quad n = +1, +2, +3, \dots \quad (5.10b)$$

Also we get

$$\left. \frac{d\alpha}{d\tau} \right|_{\alpha=0} = \frac{\beta(\beta - \omega)}{[1 \pm K\tau]^2 + [K\tau \sin(\beta\tau)]^2}. \quad (5.11)$$

Hence, as in the case of the single oscillator,

$$\frac{d\alpha}{d\tau} \Big|_{\alpha=0} \begin{cases} < 0 \text{ on } \tau_1 & \text{if } K < f(\omega), \\ > 0 \text{ on } \tau_1 & \text{if } K > f(\omega), \\ = 0 \text{ on } \tau_1 & \text{if } K = f(\omega), \\ > 0 & \text{on } \tau_2 \end{cases} \quad (5.12)$$

where $f(\omega) = \sqrt{1 + \omega^2}$. In analogy with the arguments as in the case of single limit cycle oscillator with the delay feedback, there exists only a single death island enclosed between the critical curves $\tau_1(0, K)$ and $\tau_2(1, K)$ for small values of ω . However, for large values of ω , one can obtain the higher order islands as demonstrated [7–10] above.

The results have also been extended to the case of a large assembly of delay coupled limit cycle oscillators with global [7, 8, 10] and ring [11] coupling configuration in order to show the general nature of amplitude death phenomenon. The same authors have also provided experimental evidence for the existence of delay induced death phenomenon in two delay coupled limit cycle oscillators using electronic circuits, which will be discussed in detail in the next section.

5.2.2 Experimental Study

Experimental observation of time-delay induced amplitude death in two coupled limit cycle oscillators has also been reported by Ramana Reddy et al. [9]. They have provided experimental evidence for time-delay induced death islands and their multiple connectedness as predicted by their theoretical studies in the parameter space defined by the coupling strength, time-delay and frequency for the case of two coupled identical limit cycle oscillators using a suitable electronic circuit.

A schematic representation of the system of two coupled electronic circuits that are individually capable of exhibiting limit cycle oscillations is shown in Fig. 5.2. Each individual oscillator circuit is a nonlinear LCR circuit, which may be considered as a variant of the well known Chua circuit. Each one of these circuits consists

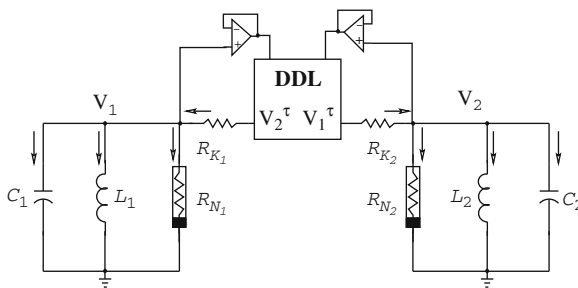


Fig. 5.2 The circuit diagram of two delay coupled nonlinear LCR circuits that are capable of exhibiting limit cycle oscillations [9]

of a capacitance C , an inductance L and a nonlinear resistive element R_N that are coupled through a digital delay line (DDL). The OP-AMPs are buffer amplifiers and the coupling strength $K = 1/(CR_K)$ is varied by changing the resistances R_K that couple the two oscillator circuits. The coupling is linear, resistive, and proportional to the difference in the signal strengths of the two oscillators with a time-delay. Each oscillator is capable of oscillating with a characteristic frequency $\omega = 1/\sqrt{LC}$. The authors have fixed the values of capacitances as $C_1 = C_2 = 0.1 \mu F$ and the values of the inductances $L = L_1 = L_2$ and the resistances $R = R_{K1} = R_{K2}$ are varied

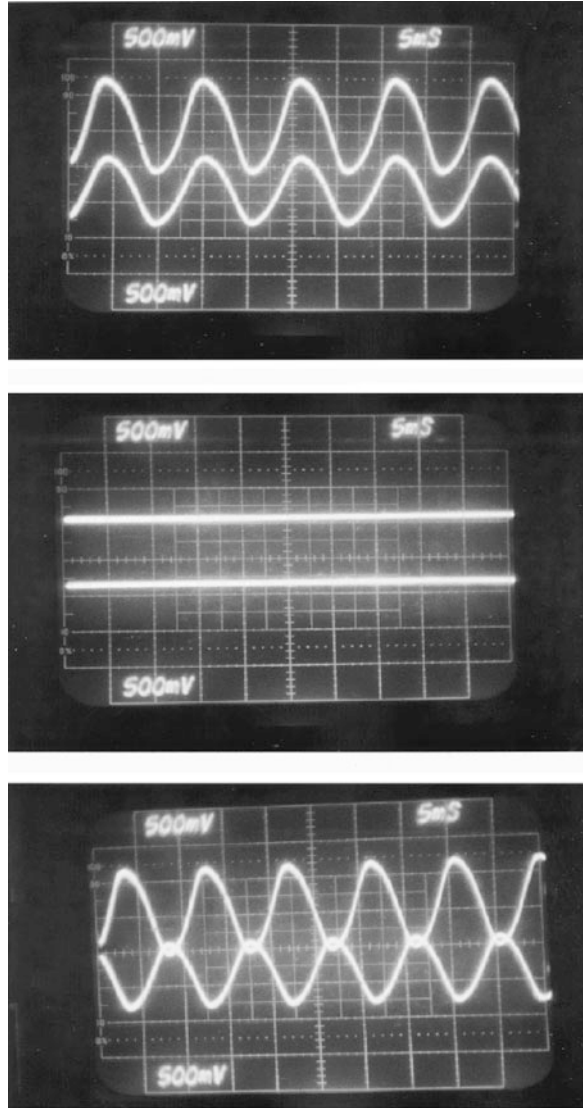


Fig. 5.3 Experimental results of two delay coupled limit cycle oscillators for different values of delay times with $K = 1,000/s$ and $\omega = 837 s$. The *top panel* shows the in-phase oscillations for $\tau = 0.514 ms$, the *middle panel* shows amplitude death for $\tau = 2 ms$ and the *bottom panel* displays anti-phase oscillations for $\tau = 4.428 ms$. This figure is adapted from the work of Ramana Reddy et al. [9]

such that the frequencies $\omega = \omega_1 = \omega_2$ and the coupling strengths $K = K_1 = K_2$ vary in the ranges of 100–1,000/s and 10–10⁶/s, respectively.

The experimental results of the time evolution of the oscillator voltages as a function of the delay parameter are shown in Fig. 5.3 for $K = 1,000$ /s and $\omega = 837$ /s. In-phase oscillations of the coupled identical limit cycle oscillators are shown in the top panel of Fig. 5.3 for $\tau = 0.514$ ms. Quenching of oscillations, that is, amplitude death is observed for $\tau = 2$ ms as shown in the middle panel of Fig. 5.3 and anti-phase oscillations are observed for $\tau = 4.428$ ms as depicted in the bottom panel of Fig. 5.3. Thus the phenomenon of time-delay induced amplitude death has been experimentally observed in coupled identical nonlinear LCR circuits with delay feedback for suitable values of the experimental parameters.

Amplitude death has also been shown to occur in a dual-wavelength class-B laser with modulated losses by Kuntsevich and Pisarchik [12], which is a nonautonomous system since the losses in a channel are modulated by an external sinusoidal force.

The phenomenon of amplitude death has also been reported experimentally [13] in a pair of opto-thermal oscillators that are coupled by heat transfer. Existence of amplitude death for stronger couplings and its relation to Hopf bifurcations of the uncoupled and coupled systems have also been experimentally verified. The authors of [13] have also complimented their experimental results with a theoretical analysis of the corresponding model equations. However, the role of delay in the death phenomenon in this experiment has not been clearly understood.

5.3 Amplitude Death with Distributed Delay in Coupled Limit Cycle Oscillators

F.M. Atay [14] has shown that distributed delay increases the parameter regime in which the phenomenon of amplitude death occurs. He has demonstrated that distributed delay enlarges and merges death islands and the death region becomes unbounded if the variance of the delay distribution is larger than a certain threshold. Since most of the studies are concerned with constant or discrete delays, propagation of information among the corresponding physical systems occurs only at fixed time intervals while the dynamical systems themselves are evolving. In contrast, physical systems in such situations can be better understood if the propagation delay from one unit to the other is also evolving dynamically or uniformly distributed over an interval. This approach is particularly significant in biological systems (in particular in neurobiology) where the system can be described by networks of coupled dynamical units evolving in time, for instance as in the case of evolving networks.

Realizing the importance of time-delay in inducing amplitude death in identical limit cycle oscillators, now we will discuss briefly the effects of distributed delay on these systems. Atay has considered a system of two coupled limit cycle oscillators, each one of the form of Eq. (5.1), with a distributed delay coupling [14]. The dynamical equation can be written as

$$\dot{Z}_1(t) = (1 + i\omega - |Z_1(t)|^2)Z_1(t) + K \left[\int_0^\infty f(\tau')Z_2(t - \tau')d\tau' - Z_1(t) \right], \quad (5.13a)$$

$$\dot{Z}_2(t) = (1 + i\omega - |Z_2(t)|^2)Z_2(t) + K \left[\int_0^\infty f(\tau')Z_1(t - \tau')d\tau' - Z_2(t) \right], \quad (5.13b)$$

where K is the coupling strength and f represents the distribution of delay time. In particular, the distributed delay is considered to be uniformly distributed over the interval $\tau \pm \delta$, that is $f(\tau)$ in the above Eq. (5.13) has been chosen as

$$f(\tau) = \begin{cases} \frac{1}{2\delta}, & |\tau - \tau'| \leq \delta \\ 0, & \text{else} \end{cases} \quad (5.14)$$

Carrying out a linear stability analysis about the fixed point $Z = 0$ in Eq. (5.13), as discussed in Sect. 2.4, and in the previous section, one can obtain the pair of stability curves as

$$(1 - \gamma^2)K^2 - 2K + 1 = -(\beta - \omega)^2, \quad (5.15)$$

$$\tan(\beta\tau) = \frac{\beta - \omega}{1 - K}, \quad (5.16)$$

where

$$\gamma = \gamma(\beta, \delta) = \begin{cases} \sin(\beta\delta)/(\beta\delta), & \beta\delta \neq 0 \\ 1, & \beta\delta = 0. \end{cases} \quad (5.17)$$

The stability regime confined by the above critical curves in the (τ, K) parameter space is again determined from the knowledge of $Re(d\lambda/d\tau)$ on the critical curves as was done in the previous section. The stability regime in the (τ, K) space for the value of the parameter $\omega = 30$ is shown in Fig. 5.4 for the above mentioned uniformly distributed delay for various values of δ . For the value of $\delta = 0.0$ the distributed delay becomes a discrete delay and the corresponding stability regime for this parameter value consists of three amplitude death islands, Fig. 5.4a, which continuously deforms as the degree of distribution determined by the value of the parameter δ increases as seen in Fig. 5.4b–d. The connected stability regimes become unbounded in the direction of the delay time τ after certain threshold value of δ , Fig. 5.4c, d.

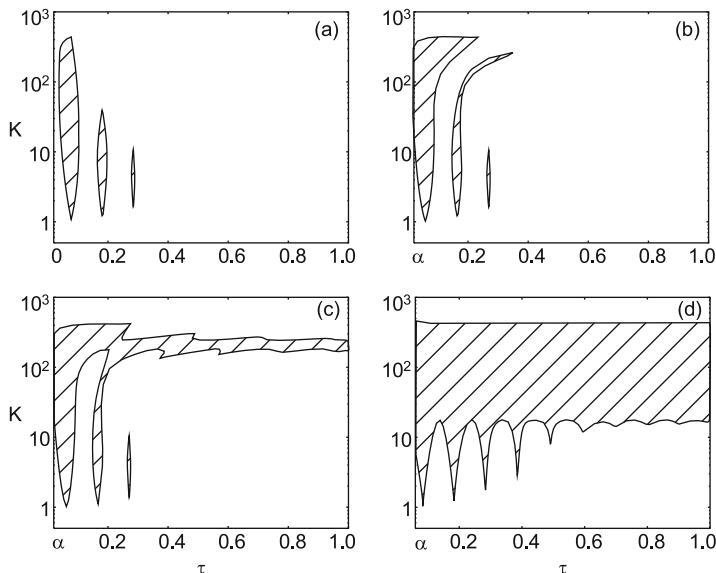


Fig. 5.4 Spread of amplitude death islands as the distribution of the delay increases. (a) $\delta = 0$, (b) $\delta = 0.007$, (c) $\delta = 0.008$ and (d) $\delta = 0.02$. This figure is adapted from the work of F. M. Atay [14]

5.4 Amplitude Death in Coupled Chaotic Oscillators

In the previous sections, we have discussed the phenomenon of amplitude death in a single/coupled limit cycle oscillator driven autonomously by a time-delay feedback and also in two coupled limit cycle oscillators with distributed delay. We also note that this phenomenon has been shown to occur in a large ensemble of coupled limit cycle oscillators with time-delay coupling [8, 10]. It has also been demonstrated that this phenomenon is generic and that it can also occur in chaotic dynamical systems with time-delay coupling, similar to the case of coupled limit cycles. As this phenomenon is quite general, it occurs for identical as well as nonidentical coupled chaotic systems. The existence of amplitude death with time-delay coupling has been discussed in coupled Lorenz and Rössler chaotic oscillators by A. Prasad [15].

It has also been shown that the transition from chaos to amplitude death via a limit cycle occurs in analogy with the same mechanism as that of the coupled limit cycle oscillators [3, 7, 8], that is, a pair of complex conjugate eigenvalues cross the imaginary axis from right to left and simultaneously the unstable fixed point becomes stable, initiating the amplitude death at a Hopf bifurcation. However there exist two distinct nature of transitions to the fixed point from the limit cycle behavior, namely in-phase and out-of-phase transitions. The shift in the nature of these distinct transitions occurs at a critical value of delay time τ_c at which the phase relationship of the two oscillators changes from in-phase to out-of-phase oscillations

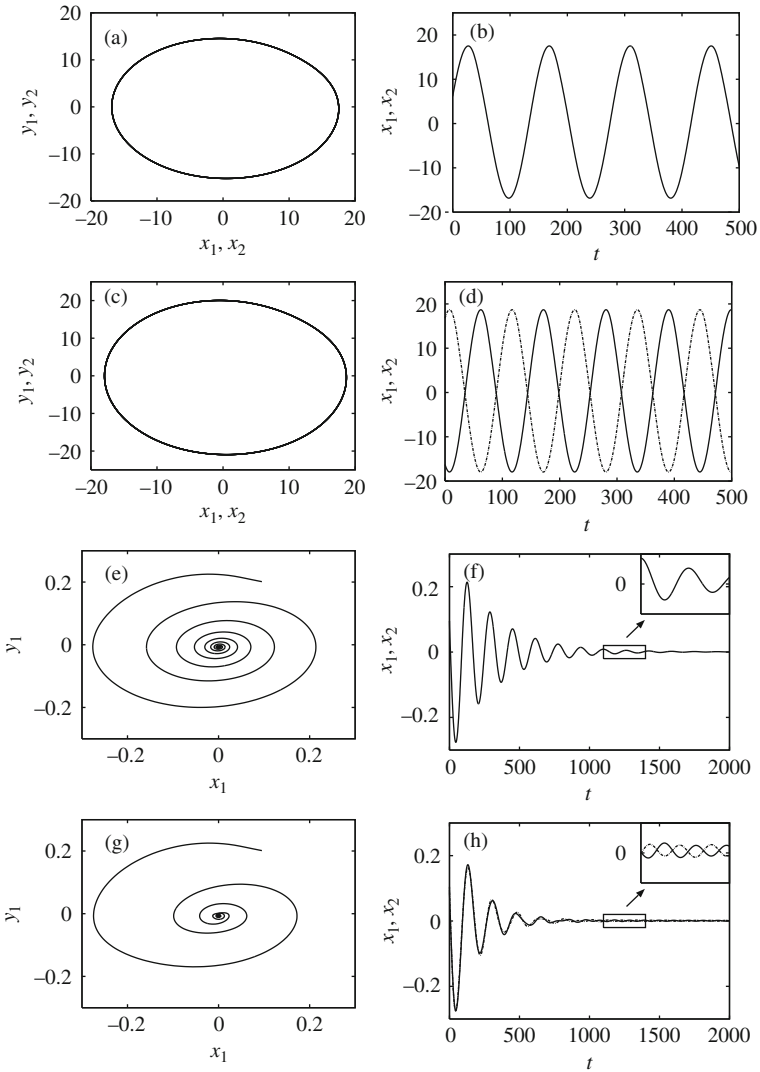


Fig. 5.5 Phase space plots (*left panel*) and time series plots (*right panel*) of the coupled identical Rössler oscillators (5.18). (a) and (b) at $\tau = 0.6$, (c) and (d) at $\tau = 2.25$, (e) and (f) at $\tau = 1.5$ and (g) and (h) at $\tau = 2$, respectively, see [15]

as a function of delay time τ . These distinct transitions were later realized as a *phase flip* bifurcation [16] which is discussed below.

To be specific, consider a system of two delay coupled identical Rössler oscillators [15] represented by

$$\dot{x}_i = -y_i - z_i, \quad (5.18a)$$

$$\dot{y}_i = x_i + ay_i + \varepsilon(y_j(t - \tau) - y_i), \quad (5.18b)$$

$$\dot{z}_i = b + z_i(x_i - c), \quad i, j = 1, 2, i \neq j, \quad (5.18c)$$

where $a = b = 0.1$, $c = 14$, $\varepsilon = 0.5$ and the delay time τ is considered as the control parameter. In the absence of coupling $\varepsilon = 0$, the individual systems (5.18) evolve chaotically for the above values of the parameters. Dynamical behavior of the coupled identical Rössler oscillators for various values of time-delay τ are shown in Fig. 5.5. Limit cycle oscillations of both the coupled systems are shown in Fig. 5.5a for the delay time $\tau = 0.6$ and the corresponding time series plot is depicted in Fig. 5.5b, where there is no phase difference between both the oscillators x_1 and x_2 . This implies that both the oscillators x_1 and x_2 are exhibiting in-phase oscillations. Similar limit cycle oscillations and their time trajectory plots of both the coupled oscillators are illustrated in Fig. 5.5c, d, respectively, for the value of delay time $\tau = 2.25$. In contrast to the previous case, it can be now noted from the time series plot that the variables x_1 and x_2 exhibit out-of-phase oscillations. For the value of delay time $\tau = 1.5$, the coupled chaotic oscillators transit to their fixed point as shown in Fig. 5.5e, f, where the oscillators are in in-phase state which can be seen clearly in the inset of Fig. 5.5f. Transition to the fixed point of both the oscillators by out-of-phase oscillations for the value of time-delay $\tau = 2$ is depicted in Fig. 5.5g, h. These distinct transitions from in-phase to out-of-phase oscillations can also be identified from the phase-difference ($\Delta\phi$) between the two oscillators defined as $\Delta\phi = \langle |\phi_1(t) - \phi_2(t)| \rangle$, where $\langle \cdot \rangle$ denotes the time average while $\phi = \arctan(y/x)$. The phase-difference ($\Delta\phi$) between the two oscillators as a function of the delay time $\tau \in (0, 2.5)$ is shown in Fig. 5.6.

These distinct transitions to amplitude death via limit cycle oscillations and their mechanism of transitions in coupled chaotic oscillators are generic in nature and that they can also be demonstrated in coupled identical Lorenz oscillators, coupled non-identical Rössler and Lorenz oscillators and also in mixed chaotic oscillators [15].

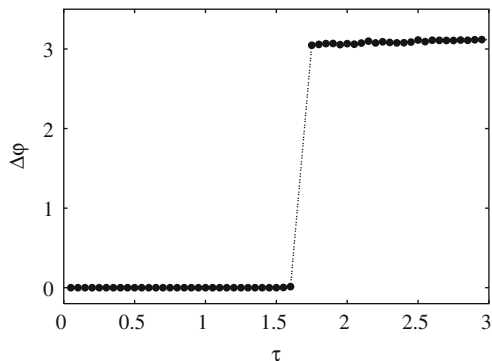


Fig. 5.6 Phase difference $\Delta\theta = \langle |\theta_1(t) - \theta_2(t)| \rangle$ (which before and after the transition are equal to 0 and π) between the oscillators, (5.18), as a function of delay time in the range $\tau \in (0, 3)$

5.5 Amplitude Death with Conjugate (Dissimilar) Coupling

Recently, it was shown that amplitude death can also occur by coupling through conjugate (dissimilar) variables [17]. The scenario for the occurrence of amplitude death in this case is quite different from our previous discussions in time-delay coupled set of identical oscillators. In [17] it has been demonstrated that amplitude death can occur in identical limit cycle oscillators, and even in identical chaotic oscillators, with conjugate coupling without time-delay. It was realized that coupling via conjugate variables provides time-delayed interaction in the sense that the other variables of a dynamical system are reconstructed from a known time series using a time-delay, a procedure in embedding. Indeed Takens' embedding theorem [18] asserts that the topological properties of the reconstructed system match those of the true system for suitable choices of embedding dimension and time-delay. The similarity between time-delayed variables and conjugate variables has been extensively employed in the process of attractor reconstruction [19]. Hence, the analysis of [17] asserts that some of the time-delay coupling effects can also be realized by means of conjugate coupling and this reduces computing efforts enormously when arrays or networks of oscillators are considered. It is also to be noted that it is easy to implement conjugate coupling in experiments when compared to time-delay feedback or coupling. However, the conjugate coupling does not lead to the infinite dimensionality of a dynamical system thereby leading to hyperchaotic attractors with large number of positive Lyapunov exponents, a hallmark property of a dynamical system with time-delay feedback or coupling.

Coupling conjugate (dissimilar) variables is natural in a variety of experimental situations where subsystems are coupled by feeding the output of one into the other. As an example for employing the conjugate coupling, recently Kim et al. [20] in their experiments on coupled semiconductor laser systems used photon intensity fluctuation from one laser to the other to modulate the injection current and vice versa.

Consider, as an example, the Landau-Stuart oscillator specified by the equation of motion

$$\dot{Z}(t) = (1 + i\omega - |Z(t)|^2)Z(t), \quad (5.19)$$

where ω is the frequency and $Z(t) = x(t) + iy(t)$. Two such dynamical equations coupled through conjugate (dissimilar) variables can be expressed in Cartesian coordinates as

$$\dot{x}_i(t) = P_i x_i - \omega_i y_i, \quad (5.20a)$$

$$\dot{y}_i(t) = P_i y_i + \omega_i x_i + \varepsilon x_j, \quad (5.20b)$$

where $P_i = 1 - |Z_i|^2$, $i, j = 1, 2$, and $j \neq i$, ε is the coupling strength and $\omega_i = \omega = 2.0$. The largest Lyapunov exponent of the coupled system (5.20) is shown in Fig. 5.7 in the range of coupling strength $\varepsilon \in (1, 3)$. For $\varepsilon < 2$, the largest

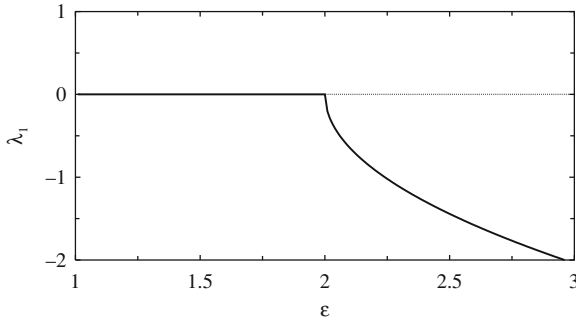


Fig. 5.7 Largest Lyapunov exponent of the coupled Landau-Stuart oscillator (5.20) as a function of the coupling strength in the range $\varepsilon \in (1, 3)$

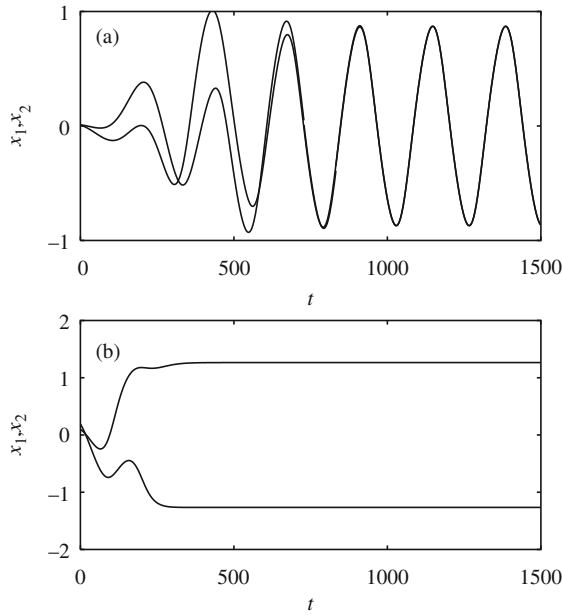


Fig. 5.8 Trajectories of the x components of the two oscillators (5.20). (a) Limit cycle behavior for the coupling strength $\varepsilon = 1.0$, and (b) Monotonic decay to the fixed points for $\varepsilon = 2.5$

Lyapunov exponent is zero and the second largest one is negative (which is not shown here), which is indicative of the limit cycle behavior as shown in Fig. 5.8a. For $\varepsilon > 2$, transient trajectories decay monotonically to the fixed points as shown in Fig. 5.8b for the value of the coupling strength $\varepsilon = 2.5$.

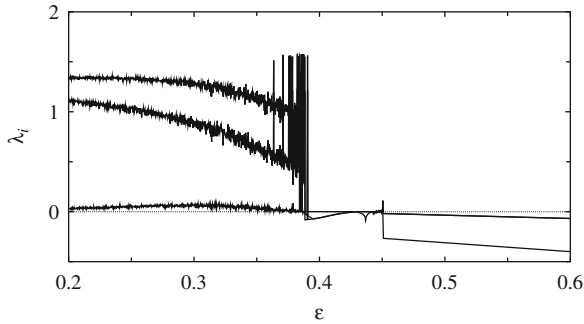


Fig. 5.9 Largest three Lyapunov exponents of the coupled Lorenz systems (5.21) as a function of the coupling strength in the range $\varepsilon \in (0.2, 0.6)$

It has also been shown that amplitude death occurs in coupled Lorenz oscillators coupled through conjugate variables [17],

$$\dot{x}_i = 10(-y_i - x_i), \quad (5.21a)$$

$$\dot{y}_i = -x_i z_i + 28x_i - y_i + \varepsilon(x_j - y_i), \quad (5.21b)$$

$$\dot{z}_i = x_i y_i - \frac{8}{3}z_i, \quad i, j = 1, 2, i \neq j. \quad (5.21c)$$

The largest three Lyapunov exponents of the coupled Lorenz system is depicted in Fig. 5.9 as a function of the coupling strength $\varepsilon \in (0.2, 0.6)$. All the Lyapunov exponents become negative for $\varepsilon > 0.44$, indicating the occurrence of amplitude death in the coupled Lorenz system. Preceding the regime of amplitude death the largest Lyapunov exponents show wild fluctuations due to the presence of coexisting attractors, namely multistability, an impact of time-delay. Chaotic trajectories of both the coupled Lorenz systems for the value of the coupling strength $\varepsilon = 0.3$ is shown in Fig. 5.10a, while the dynamical behavior in the amplitude death regime is plotted in Fig. 5.10b for the value of the coupling strength $\varepsilon = 0.5$.

5.6 Amplitude Death with Dynamic Coupling

In the above studies on amplitude death, the coupling signal is proportional to the difference between the dissimilar or conjugate states of the two oscillators. The proportionality factor is of a constant value and hence the couplings are considered *static*. It was observed that *dynamic* coupling, which has not only the proportionality factor but also has its own dynamics, can induce amplitude death without time-delay [21]. It is to be noted that RC-ladder coupling [22], a kind of dynamic coupling, can be used as an approximation of RC wire delay connections in VLSI

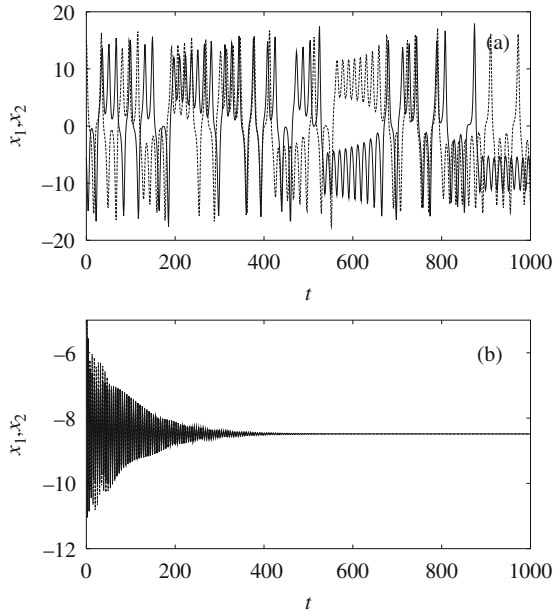


Fig. 5.10 Transient trajectories of the x components of the coupled Lorenz systems (5.21). (a) Chaotic behavior for $\varepsilon = 0.3$ and (b) Monotonic decay to the fixed points for $\varepsilon = 0.5$

chips [23]. Consequently, dynamic coupling may also be used to produce some of the time-delay effects in appropriate situations.

To illustrate the existence of amplitude death due to dynamic coupling, let us consider the two identical limit cycle oscillators

$$\dot{x}_i = x_i \left(1 - y_i^2 - x_i^2 \right) - \omega y_i + u_i, \tag{5.22a}$$

$$\dot{y}_i = y_i \left(1 - y_i^2 - x_i^2 \right) - \omega x_i, \quad i = 1, 2, \tag{5.22b}$$

where the dynamic coupling involves an additional variable with a time evolution,

$$\dot{z}_i = -z_i + x_j, \quad u_i = \varepsilon(z_i - x_i) \quad i, j = 1, 2, i \neq j, \tag{5.23}$$

where ε is the coupling strength. The limit cycle oscillations of the coupled system is shown in Fig. 5.11a in the absence of coupling, that is $\varepsilon = 0$. As the value of the coupling strength is increased from zero for a fixed value of the natural frequency $\omega = 4$, oscillatory behavior is found to exist up to a certain threshold value of the coupling strength, followed by a sudden quenching of oscillations above the threshold value, leading to amplitude death of the oscillators. The full scenario is shown as a bifurcation diagram in Fig. 5.12 as a function of the coupling strength in the range $\varepsilon \in (0, 12)$. Both the oscillators exhibit chaotic oscillations in the range $\varepsilon \in (0, 2.3)$ and amplitude death occurs in the range $\varepsilon \in (2.3, 8.5)$, where all the variables converge to the origin. The stable fixed point, which differs from

Fig. 5.11 Behavior of the system of coupled limit cycle oscillators (5.22), (5.23). (a) Limit cycle oscillations of the two uncoupled systems in the absence of coupling, (b) Quenching of oscillations (amplitude death) of the coupled oscillators for the value of the coupling strength $\varepsilon = 4.0$ and (c) Both the limit cycle oscillations and quenching of oscillations before and after the dynamic coupling, respectively, switched at $t = 1500$

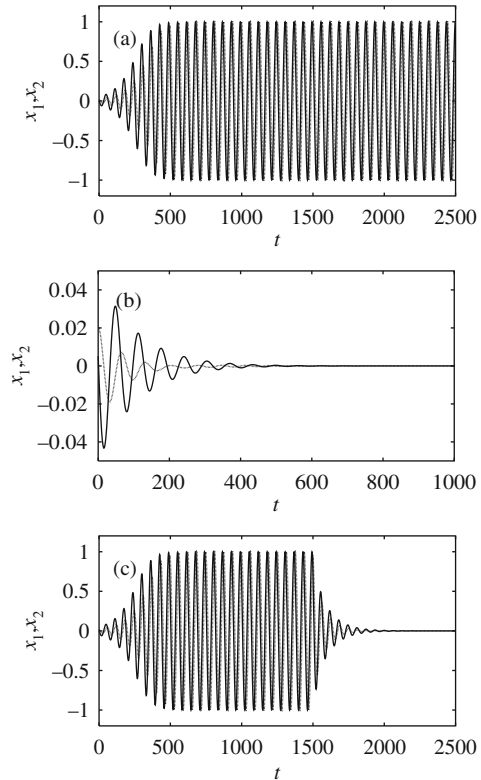
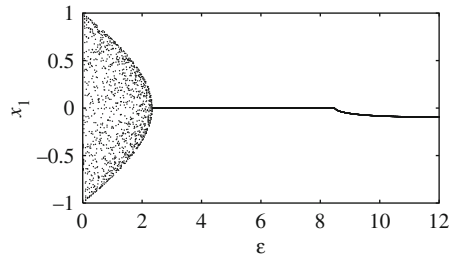


Fig. 5.12 Bifurcation diagram of the coupled limit-cycle oscillators (5.22), (5.23) as a function of the coupling strength $\varepsilon \in (0, 12)$ for a fixed value of frequency $\omega = 4.0$



the origin, appears for $\varepsilon > 8.5$. Figure 5.11b shows the limit cycle oscillations being damped out to reach the fixed point for $\varepsilon = 4.0$, while Fig. 5.11c shows the existence of the limit cycle oscillations and quenching of oscillations, respectively, before and after the dynamic coupling is switched on at $t = 1500$. Quenching of oscillations due to dynamic coupling can also be demonstrated in coupled identical Rössler systems [21].

Recently, the phenomenon of amplitude death has also been reported in coupled time-delay systems [24] with both delay and dynamic couplings. Stability condition for the stabilization of the oscillatory behavior in coupled time-delay systems has

also been derived and it is also shown that static connection never induces amplitude death. These results have also been confirmed experimentally using electronic circuits.

5.7 Time-Delay Induced Bifurcations

It has also been shown that phase flip bifurcation occurs in a general class of nonlinear oscillators coupled through time-delay coupling [16]. Here, the relative phase between the coupled oscillators changes abruptly from zero to π as a function of the delay time for fixed values of the other system parameters and hence it is named as a phase flip bifurcation, which is a general feature of the time-delay coupled systems. This bifurcation phenomenon has a broad range of occurrence, that is, it is observed for periodic as well as chaotic oscillators, for identical as well as nonidentical coupled systems, and in a variety of dynamical systems [16].

For illustration, let us consider a pair of diffusively coupled Rössler oscillators represented by Eqs. (5.18) with the same values of the parameters a , b and c as used in the Sect. 5.4. They evolve chaotically as indicated in Sect. 5.4. The coupling strength ε and delay time τ are chosen as control parameters. The phase difference $\Delta\phi = \langle |\phi_1(t) - \phi_2(t)| \rangle$, where $\langle \cdot \rangle$ is the time average, is depicted in Fig. 5.13 in the (ε, τ) parameter space. From this figure it is evident that the relative phase between both of the coupled systems is zero for a fixed value of the coupling strength ε up to a certain threshold value of delay time τ and above this threshold value there is a difference of π in the relative phase. As the phase flips from zero to π as a function of the delay time, this phenomena is termed as phase flip bifurcation. The dynamics of this phase flip bifurcation, namely transition from in-phase oscillations to out of phase oscillations has been discussed in Sect. 5.4 (see Fig. 5.5) for both limit cycle oscillations and chaotic oscillations.

It was also observed that Neimark-Sacker-type bifurcation [25] is prevalent in delay coupled networks for larger values of delay times, which results in high-period solutions followed by more complex behavior [26]. It was shown that the synchronized solution of delay coupled logistic map exhibits such complex bifurcation

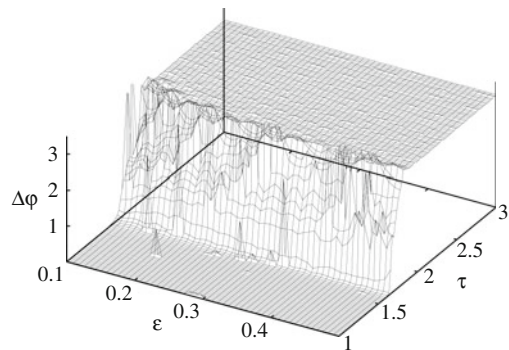


Fig. 5.13 Phase difference $\Delta\phi$ in the (ε, τ) plane

scenario for finite values of connection delays whereas such bifurcation scenario (Neimark-Sacker-type bifurcation) cannot arise in one-dimensional maps [26], a clear implication of delay coupling. It has also been shown that a variety of rich bifurcation structures can arise in the synchronized solution as a function of the coupling strength for finite values of connection delays.

Bifurcations such as inverse, direct Hopf and fold limit cycle were observed in time-delay coupled FitzHugh-Nagumo excitable systems [27]. It was also identified that for an intermediate range of time lags, inverse sub-critical Hopf and fold limit cycle bifurcations lead to the phenomenon of oscillator death [27]. Bifurcations in two coupled excitable FitzHugh-Nagumo systems ($N = 2$) has been studied analytically, and it is also numerically confirmed that the same bifurcations are relevant for $N > 2$ in the presence of delay coupling.

5.8 Some Other Effects of Delay Feedback

In the following, we will briefly point out the main features and the emergence of other types of behaviors in delay coupled systems (delay feedback) which are not possible in the absence of time-delay feedback.

1. The first systematic investigation of time-delayed coupling was done by Schuster and Wagner [28] who studied two coupled phase oscillators and found multistability of synchronized solutions.
2. A novel form of frequency depression was observed for small delays in the limit cycle oscillators that interact via time-delayed diffusive coupling and for larger delay metastable synchronized state was observed [29].
3. Bistability between synchronized and incoherent states have been observed in Kuramoto oscillators coupled via time-delay coupling. Exact formulas for the stability boundaries of the incoherent and synchronized state as a function of the delay has been established [30].
4. Delay induced chaos has been demonstrated in catalytic surface reaction [31]. A mathematical model has been proposed which explains the origin of chaos in this reaction as being due to delays in the response of a population of reacting adsorbate islands globally coupled via the gas phase. The dynamical equations of this model yields a sequence of period-doubling bifurcations resulting in chaos [31].
5. It has also been shown that delay coupling in networks enhances the synchronizability of networks and interestingly it leads to the emergence of a wide range of new collective behavior (see [26, 32] and reference therein). On the other hand, it has also been shown that connection delays can actually be conducive to synchronization so that it is possible for delayed systems to synchronize whereas the undelayed system does not [26].
6. Enhancement of neural synchrony, that is, the existence of stable synchronized state even for a very low coupling strength for significant time-delay in the coupling has also been demonstrated [33].

7. Time-delay feedback has also been demonstrated to be used for bifurcation control of nonlinear models of chaotic cardiac activity [34].
8. It has also been demonstrated that time-delay feedback can be used for suppressing a pathological period-2 rhythm (cardiac alternans) in an atrioventricular nodal conduction model [35].
9. In delay coupled fiber lasers, it was demonstrated that a reduction in dynamical complexity occurs for short coupling delays while a logarithmic growth is observed as the coupling delay is increased [36].

References

1. K. Bar-Eli, J. Phys. Chem. **94**, 2368 (1990)
2. M. Shiino, M. Frankowicz, Phys. Lett. A **136**, 103 (1989)
3. D.G. Aronson, G.B. Ermentrout, N. Koppel, Physica D **41**, 403 (1990)
4. K. Okuda, Y. Kuramoto, Prog. Theor. Phys. **86**, 1159 (1991)
5. G.B. Ermentrout, Physica D **41**, 219 (1990)
6. R.E. Mirollo, S.H. Strogatz, J. Stat. Phys. **60**, 245 (1990)
7. D.V. Ramana Reddy, A. Sen, G.L. Johnston, Phys. Rev. Lett. **80**, 5109 (1998)
8. D.V. Ramana Reddy, A. Sen, G.L. Johnston, Physica D **129**, 15 (1999)
9. D.V. Ramana Reddy, A. Sen, G.L. Johnston, Phys. Rev. Lett. **85**, 3381 (2000)
10. D.V. Ramana Reddy, Ph. D. Thesis entitled *Collective Dynamics of Delay Coupled Oscillators* (Institute for Plasma Research, Gandhinagar, India, 2000)
11. R. Dodla, A. Sen, G.L. Johnston, Phys. Rev. E **69**, 056217 (2004)
12. B.F. Kuntsevich, A.N. Pisarchik, Phys. Rev. E **64**, 046221 (2001)
13. R. Herrero, M. Figueras, J. Rius, F. Pi, G. Orriols, Phys. Rev. Lett. **84**, 5312 (2000)
14. F.M. Atay, Phys. Rev. Lett. **91**, 094101 (2003)
15. A. Prasad, Phys. Rev. E **72**, 056204 (2005)
16. A. Prasad, J. Kurths, S.K. Dana, R. Ramaswamy, Phys. Rev. E **74**, 035204(R) (2006)
17. R. Karnatak, R. Ramaswamy, A. Prasad, Phys. Rev. E **76**, 035201(R) (2007)
18. F. Takens, in *Detecting Strange Attractors in Turbulence*, ed. by D. Rand, L. Young. Lecture Notes in Mathematics (Springer, New York, 1981)
19. N.H. Packard, J.P. Crutchfield, J.D. Farmer, R.S. Shaw, Phys. Rev. Lett. **45**, 712 (1980)
20. M.Y. Kim, R. Roy, J.L. Aron, T.W. Carr, I.B. Schwartz, Phys. Rev. Lett. **94**, 088101 (2005)
21. K. Konishi, Phys. Rev. E **68**, 067202 (2003)
22. J.P. Fishburn, C.A. Schevon, IEEE Trans. Circuits Syst. I : Fundam. Theory Appl. **42**, 1020 (1995)
23. X. Zhan, IEEE Circuits Devices Mag. **12**, 12 (1996)
24. K. Konishi, K. Senda, H. Kokame, Phys. Rev. E **78**, 056216 (2008)
25. S.N. Elaydi, *Discrete Chaos* (Chapman & Hall/CRC, Boca Raton, FL, 2000)
26. F.M. Atay, J. Jost, Phys. Rev. Lett. **92**, 044101 (2004)
27. N. Buric, D. Todorovic, Phys. Rev. E **67**, 066222 (2003)
28. H.G. Schuster, P. Wagner, Prog. Theor. Phys. **81**, 9392 (1987)
29. E. Niebur, H.G. Schuster, D.M. Kammen, Phys. Rev. Lett. **67**, 2753 (1991)
30. M.K. Stephen Yeung, H.G. Schuster, Phys. Rev. Lett. **82**, 648 (1999)
31. N. Khrustova, G. Veser, A. Mikhailov, Phys. Rev. Lett. **75**, 3564 (1995)
32. C. Massoller, A.C. Marti, Phys. Rev. Lett. **94**, 134102 (2005)
33. M. Dhamala, V.K. Jirsa, M. Ding, Phys. Rev. Lett. **92**, 074104 (2004)
34. M.E. Brandt, G. Chen, IEEE Trans. Circuits Syst. I : Fundam. Theory Appl. **44**, 1031 (1997)
35. M.E. Brandt, H.T. Shih, G. Chen, Phys. Rev. E **56**, 1334(R) (1997)
36. A.L. Franz, R. Roy, L.B. Shaw, I.B. Schwartz, Phys. Rev. Lett. **99**, 053905 (2007)